Giant permanent dipole moment of two-dimensional excitons bound to a single stacking fault

Todd Karin, Xiayu Linpeng, M. M. Glazov, M. V. Durnev, E. L. Ivchenko, Sarah Harvey, Ashish K. Rai, Arne Ludwig, Andreas D. Wieck, and Kai-Mei C. Fu

Phys. Rev. B **94**, 041201 — Published 25 July 2016

DOI: 10.1103/PhysRevB.94.041201

Giant permanent dipole moment of 2D excitons bound to a single stacking fault

Todd Karin,[1,*] Xiayu Linpeng,[1,*] M.M. Glazov,[2] M.V. Durnev,[2] E.L. Ivchenko,[2]
Sarah Harvey,[1] Ashish K. Rai,[3] Arne Ludwig,[3] Andreas D. Wieck,[3] and Kai-Mei C. Fu[1,4]

[1]*Department of Physics, University of Washington, Seattle, Washington 98195, USA*
[2]*Ioffe Institute, 194021 St.-Petersburg, Russia*
[3]*Lehrstuhl für Angewandte Festkörperphysik, Ruhr-Universität Bochum, D-44870 Bochum, Germany*
[4]*Department of Electrical Engineering, University of Washington, Seattle, Washington 98195, USA*

(Dated: July 1, 2016)

We investigate the magneto-optical properties of excitons bound to single stacking faults in high-purity GaAs. We find that the two-dimensional stacking fault potential binds an exciton composed of an electron and a heavy-hole, and confirm a vanishing in-plane hole g-factor, consistent with the atomic-scale symmetry of the system. The unprecedented homogeneity of the stacking-fault potential leads to ultra-narrow photoluminescence emission lines (with full-width at half maximum $\lesssim 80$ μeV) and reveals a large magnetic non-reciprocity effect that originates from the magneto-Stark effect for mobile excitons. These measurements unambiguously determine the direction and magnitude of the giant electric dipole moment ($\gtrsim e \cdot 10$ nm) of the stacking-fault exciton, making stacking faults a promising new platform to study interacting excitonic gases.

Introduction. The stacking fault (SF), a planar, atomically thin defect, is one of the most common extended defects in zinc-blende, wurtzite, and diamond semiconductors. A fundamental understanding of the SF potential is important for determining how the defect affects semiconductor device performance [1, 2], engineering heterostructures based on crystal phase [3–5], and providing a new two-dimensional (2D) platform for fundamental physics [6, 7]. Here we report on excitons bound to large-area, single SFs in high-purity GaAs, a unique system where SFs are easily isolated with far-field optical techniques. The atomic smoothness of the potential and extreme perfection of the surrounding semiconductor result in ultra-high optical homogeneity ($\lesssim 80$ μeV). This enables optical resolution of the SF exciton fine-structure and thus direct measurement of the giant built-in dipole moment ($\gtrsim e \cdot 10$ nm) via the magneto-Stark effect. These results indicate that the extremely-homogeneous SF potential may be promising for studies of many-body excitonic physics, including coherent phenomena [8–10], spin currents [11], superfluidity [12], long-range order [13–17], and large optical nonlinearities [18–20].

Stacking fault photoluminescence. Figure 1(a) shows a spectrally resolved confocal scan of SF structures in a GaAs epilayer, excited with an above band-gap laser (1.65 eV, 1.5 K) [21]. The image is colored red, green or blue according to three characteristic emission bands shown in Fig. 1e. The narrow-band PL at 1.493 and 1.496 eV originates from excitons, electron-hole pairs, bound to the 2D SF potential [22, 23]. The sample consists of a 10 μm GaAs layer on 100 nm AlAs on a 5 nm/5 nm AlAs/GaAs (10×) superlattice grown directly on a semi-insulating (100) GaAs substrate. Stacking fault structures nucleate near the substrate-epilayer interface during epitaxial growth [21].

The physical origin of the potential can be understood from the atomic structure of the SF defect: the lattice-plane ordering in the [111] direction of zinc-blende is modified by subtracting a layer (intrinsic SF, see Fig. 1c) or adding a layer (extrinsic SF). The intrinsic SF can be viewed as a monolayer of wurtzite (AB AB stacking) surrounded by zinc-blende (ABC ABC stacking) [3, 24]. Due to the band offset [25–27] and spontaneous polarization at the stacking fault [28], electrons and/or holes are attracted to the SF plane. While useful for physical motivation, this bulk phase change model must be taken with caution when applied to atomically thin SFs, which can deviate from simple theory [29]. Here, however, we find that single SFs in bulk GaAs bind excitons, confirming that the potential is attractive for at least one carrier.

In the confocal scan in Fig. 1(a), most of the SF defects appear as single triangles, which we identify as a pair of nearby SFs [30, 31]. Because the binding energy of excitons to a pair of SFs depends on the distance between the SFs [32], the PL emission energy from excitons bound to these structures has a high variability of 10 meV between structures. Strikingly, this inhomogeneity disappears when four SFs grow in an inverted pyramid structure consisting of four well-isolated {111} SF planes [Fig. 1(b)], which we refer to as *up*, *down*, *left* and *right* [33]. The full width at half-maximum (FWHM) of the SF PL line in our sample is (77 ± 19) μeV at zero magnetic field [21], somewhat narrower than excitonic lines associated with stacking faults in previous work [22, 34]. In comparison, the narrowest reported linewidth for a GaAs/AlGaAs quantum well is 130 μeV [35], while PL linewidths from analogous zinc-blende/wurtzite quantum discs in nanowires range from $0.6-10$ meV [27, 36–38]. This unprecedented homogeneity allows us to resolve the SF-bound exciton fine structure

Nature of hole in SF exciton. Experimentally, we determine that the SF exciton is composed of an electron and a heavy-hole using polarization resolved PL, consistent with the atomic-scale symmetry of the system [21]. For linearly polarized light incident from above (along the [001] axis), the largest overlap between the light polarization and the in-SF-plane heavy-hole dipole occurs when exciting and collecting along the H direction for the *down* SF [Fig. 1(d)], in agreement with our experimental data [Fig. 1(f)]. On the

* These authors contributed equally to this work.

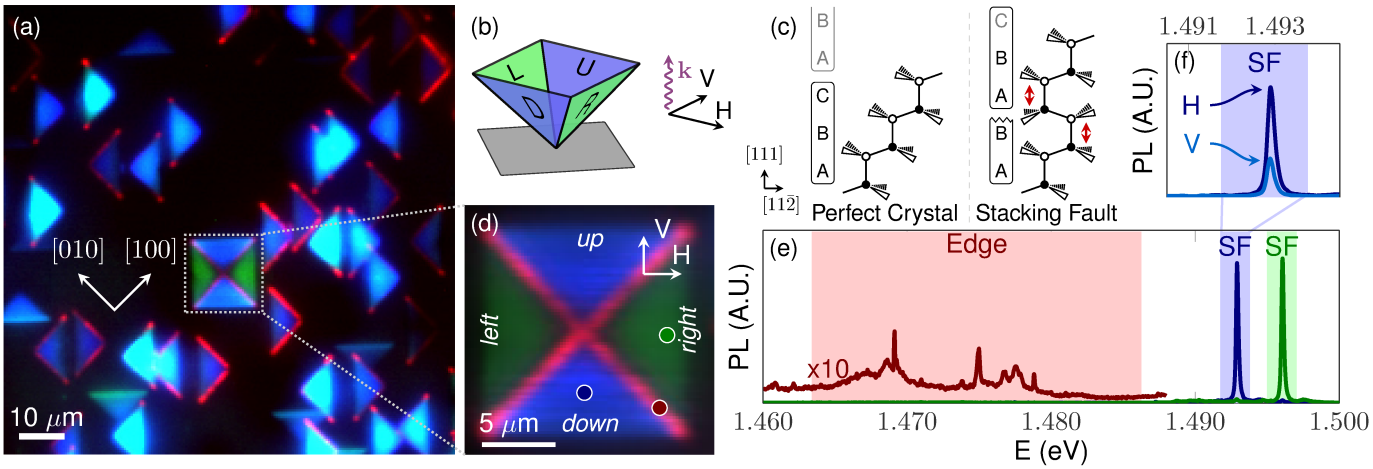

FIG. 1. (a) Confocal scan of SF structures. The image is formed by coloring emission in different wavelength bands as red, blue or green, as depicted in e. Excitation at 1.53 eV, 100 μW, 1.9 K, excite and collect H polarization (see b). (b) Diagram of SF pyramid. The *up, down, left* and *right* SFs are labeled, along with the H and V polarizations. (c) Comparison of perfect zinc-blende and stacking fault crystal structure. (d) Detail of SF pyramid structure. Excitation at 1.53 eV, 100 μW, 1.7 K. (e) Low power PL spectra at colored dots in d. Polarizations: blue - excite/collect H; green, red - excite/collect V. Broad-band luminescence is observed from the SF edges (red). 1.53 eV, 2 μW, 1.7 K. (f) PL from *down* SF (blue dot in d). Polarizations: dark blue - excite/collect H; light blue - excite/collect V.

other hand, the main dipole moment for the light-hole exciton is along the SF normal, which would give rise to a maximum signal at V polarization, contrary to what is observed. Further, we also note that no hole Zeeman splitting is observed for in-plane magnetic fields B up to 7 T (Fig. 2). This observation is fully consistent with our symmetry analysis, which finds that B-linear splitting for in-plane fields is forbidden for heavy-holes but allowed for light-holes [21]. The substantial separation of the heavy- and light-hole states prevents their magnetic-field induced mixing, in line with experiments on GaAs nanowires [21, 39].

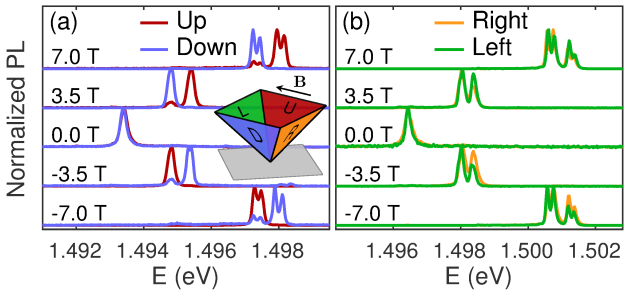

FIG. 2. (a) Spectra from *up* and *down* SFs as a function of in-plane magnetic field. The spectra show a non-reciprocity with applied magnetic field. Excite at 1.65 eV, 0.5 μW, 1.6 K, excite and collect H. Inset shows the geometry of the stacking fault pyramid and applied magnetic field. (b) Spectra from *left* and *right* SFs as a function of partially out-of-plane magnetic field. The spectra are similar at positive and negative fields. Excitation at 1.65 eV, 0.5 μW, 1.6 K, excite and collect V.

Non-reciprocal photoluminescence. PL from SFs shows a remarkable non-reciprocity with in-plane applied magnetic field: Figure 2(a) shows that the PL detected in linear polarization from the *up* SF occurs at a different energy depending on whether the magnetic field is parallel (positive) or antiparallel (negative) to the [$\bar{1}$10] axis. Interestingly, the *down* SF demonstrates the opposite behavior. Such an asymmetric behavior of the PL is surprising because in general, time reversal symmetry makes $\mathbf{B}$ and $-\mathbf{B}$ equivalent [40]. The observed non-reciprocal behavior of the PL spectrum with respect to inversion $\mathbf{B} \to -\mathbf{B}$ is only possible if the PL arises from moving excitons. In this case, time reversal changes the direction of both the magnetic field and the exciton wavevector $\mathbf{K}$.

Based on the C_{3v} point symmetry of the SF and time reversal invariance, the effective Hamiltonian for an exciton moving in the presence of an in-SF-plane magnetic field $\mathbf{B}$ is

$$\mathcal{H}_{KB} = \frac{g_e}{2}\mu_B(\sigma_x B_x + \sigma_y B_y) + \beta B^2 + \beta'[\mathbf{K}\times\mathbf{B}]_z, \quad (1)$$

where g_e is the electron g-factor, μ_B is the Bohr magneton, $\sigma_{x,y}$ are the electron spin Pauli matrices, β is a parameter describing the excitonic diamagnetic shift, and β' is a constant responsible for the non-reciprocal effect [21]. In Eq. (1) we only retain 1st- and 2nd-order terms in $\mathbf{B}$ and use a frame of axes related to the SF plane: $z \parallel [111]$ is the SF normal, $x||[11\bar{2}]$ and $y||[\bar{1}10]$. Each symmetry-derived term in Eq. (1) manifests itself in the energetic shift of the SF PL lines with magnetic field (Fig. 2). The first term is the electron Zeeman effect and gives rise to the doublets visible at ± 7 T, since an electron with a particular spin projection can recombine with the corresponding hole. The second term is the exciton diamagnetic shift, arising from the magnetic-field-induced shrinking of the exciton wavefunction [41]. The last term is the magneto-Stark effect, which, as we show below, quantitatively explains the non-reciprocal PL spectra.

The experimental geometry, Fig. 1(b), is such that only light emitted normal to the sample surface is collected. For

a high quality 2D potential, in-plane exciton momentum is transferred to the photon during recombination, as depicted in Fig. 3(a). This conservation of momentum implies

$$K_x = \frac{\omega n}{c} \sin\theta'', \tag{2}$$

where θ'' is the angle between the SF normal and the emitted photon momentum inside the semiconductor, Fig. 3(a), ω is the photon frequency, n is the refractive index and c the speed of light. Thus, the collected SF PL arises only from excitons with a specific center of mass momentum [42]. The last term in Eq. (1) provides, for a fixed K_x (Eq. 2), an odd in B_y contribution to the overall PL energy shift, giving rise to a magnetic non-reciprocity effect. It is worth noting that the *up* and *down* SFs are related by a mirror reflection in the (110) plane and such a reflection is accompanied by $B_y \to -B_y$, resulting in the opposite behavior of *up* and *down* PL spectra observed in Fig. 2(a).

Magneto-Stark effect. The physical origin of the non-reciprocal PL is the magneto-Stark effect, the interaction of a moving exciton's electric dipole moment with a magnetic field [43, 44]. The effect can be understood with a relativistic argument: motion with velocity $\mathbf{v} = (\hbar K_x/M)\hat{\mathbf{x}}$ through a magnetic field $\mathbf{B} = B_y\hat{\mathbf{y}}$ gives rise to an electric field $\mathbf{E}_{\text{eff}} = \hbar K_x B_y/(Mc)\hat{\mathbf{z}}$ in the moving frame of reference, where M is the exciton mass in translational motion and c the speed of light. Since for the SF, $\hat{\mathbf{z}} \propto [111]$ and $-\hat{\mathbf{z}}$ directions are not equivalent, the SF-bound exciton has a non-zero dipole moment $\mathbf{p} = ed_{he}\hat{\mathbf{z}}$, where $e = |e|$ is the elementary charge, and d_{he} is the average separation between the hole and electron along the z-axis. The Stark effect $H_s = -\mathbf{p}\cdot\mathbf{E}_{\text{eff}}$ in the exciton's reference frame thus becomes the magneto-Stark effect:

$$\mathcal{H}_{\text{S}} = -\frac{e\hbar}{Mc} d_{he} K_x B_y, \tag{3}$$

in agreement with Eq. (1) with $\beta' = -e\hbar d_{he}/(Mc)$, see Ref. [21, 41] for formal derivation.

Physically, the dipole moment of a SF bound exciton is a consequence of symmetry breaking and spontaneous polarization similar to that in zinc-blende/wurtzite heterostructures [23, 45]. The hole in the exciton is presumably localized in the SF plane while the electron is weakly bound via the Coulomb interaction. The spontaneous polarization shifts the electron cloud to one side of the SF, resulting in a giant excitonic dipole moment.

Equations (1)-(3) predict that the asymmetric energy shift of exciton PL is linearly related to the in-plane wavevector $\mathbf{K}$. Since the angle of light collection determines the exciton momentum [Eq. (2)], we test the applicability of the model by recording spectra of the *up* and *down* SFs as a function of the collection angle θ and magnetic field B_y [Fig. 3(b)]. The collection angle is related to the emission angle from the up/down SF by $\sin\theta = n\sin\theta' = \pm n\sin(\theta'' - \theta_{\text{SF}})$, where θ_{SF} is the angle the SF normal $\hat{\mathbf{z}}||[111]$ makes with [001] [Fig. 3(c)].

In this experiment, we modified the collection angle by mounting the sample at different angles. Since the sample was removed from the cryostat to change the angle, different SF pyramids were used at different angles. This does not introduce artifacts because of the extreme similarity of different SFs, which have a standard deviation of line-center energies of only 57 μeV, less than the linewidth. Spectra were acquired with B_y ranging from -6.5 T to 6.5 T on the *up* and *down* SFs. We fit the spectra to one or a sum of two Voigt function(s) depending on whether the electron Zeeman splitting is resolved. The singlet or doublet line center is denoted $E_{up/down}(B_y)$. The part of the exciton energy odd with magnetic field is found by computing

$$\Delta E_{up/down}(B_y) = E_{up/down}(B_y) - E_{up/down}(-B_y) \tag{4}$$

It follows from Eq. (3) that the asymmetric shift is

$$\Delta E_{up/down}(B_y) = \mp 2n\hbar\omega \frac{ed_{he}}{Mc} \sin(\theta_{SF} \pm \theta') B_y. \tag{5}$$

Thus the proportionality constant of $\Delta E_{up/down}$ vs. B_y provides a measurement of the SF exciton's built-in dipole moment. The experimental values and first-order theory for ΔE are shown in Fig. 3(f)-(g). Further, the ratio

$$r(\theta) = \frac{|\Delta E_{up}| - |\Delta E_{down}|}{\frac{1}{2}\left(|\Delta E_{up}| + |\Delta E_{down}|\right)} \tag{6}$$

depends (to first order in B_y) only on the experimental geometry and the index of refraction: $r(\theta)$ vanishes for collection angle $\theta = 0$ and increases as a function of θ [Fig. 3(h)]. We obtain good agreement between $r(\theta)$ calculated experimentally from the $B = 0$ slope of ΔE without any fit parameters [Fig. 3(h)].

Further, by fitting $\Delta E_{up/down}(B_y)$ with a B_y-linear function, we can estimate the dipole moment of the exciton $p = ed_{he} = e\cdot(10^{+20}_{-1})$ nm. The main uncertainties result from the accuracy of the B_y-linear fit and the value of the in-(111)-plane heavy-hole mass, which depends on the details of the SF potential [21]. The exciton mass can be roughly estimated as $0.17\,m_o$, the sum of the bulk-GaAs in-(111)-plane heavy-hole mass and the isotropic electron mass, where m_o is the free electron mass. In addition, we note the magneto-Stark induced splitting saturates at high fields [Fig. 3(f,g)], possibly due to a decreased exciton dipole moment from the magnetic-field-induced shrinking of the exciton wavefunction. Future work will investigate exciton confinement potentials consistent with the observed dipole moment, diamagnetic shift and saturation of the magneto-Stark effect. A microscopic understanding of the confinement potential may enable predictions for the binding potential and excitonic dipole moment for SFs in other semiconductors.

Conclusion. We have shown that SFs in GaAs are an almost perfect 2D potential which binds heavy-hole excitons. These excitons freely propagate in the SF plane, a conclusion confirmed via the magneto-Stark effect. Further, an asymmetry of the SF potential induces a giant dipole moment of the SF-bound exciton. Such excitons could be useful for studying the many-body physics of interacting dipoles. In conventional excitonic systems, typical electron-hole separations are on the order of several nm [6, 46], whereas the SF-bound exciton has a gigantic electron-hole separation of 10 nm and the possibility to modify this value with an

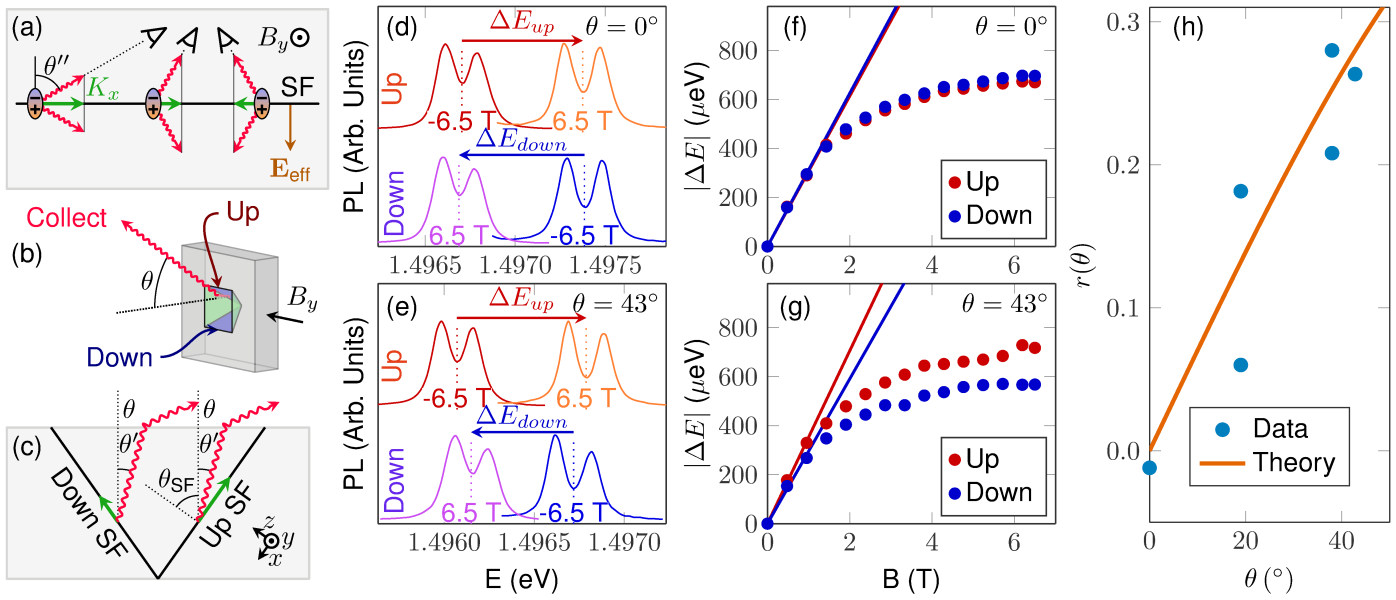

FIG. 3. (a) Because of conservation of in plane momentum during exciton recombination, the angle of light emission depends on the exciton wavevector. Collecting different angles probes different exciton momenta. The SF has a built in potential that creates a zero-field dipole moment for the SF exciton. In the exciton frame of reference, the in-plane magnetic field becomes an out-of-plane electric field, leading to the magneto-Stark effect. (b) Spectra of *up* and *down* SFs as a function of θ and in-plane magnetic field B_y. (c) Light from the *up* SF originates from excitons with larger K_x than light from the *down* SF (for $\theta > 0$). (d-e) Spectra of *up* and *down* SF at positive and negative B_y for $\theta = 0°$ and 43°. At $\theta = 0°$, ΔE_{up} and ΔE_{down} have the same magnitude, while for $\theta = 43°$, the magnitude of ΔE_{up} is larger than ΔE_{down}. (f-g) Splitting $\Delta E_{up/down}$ as a function of magnetic field. Data are obtained from Voigt fits to spectra similar to those shown in d-e. Solid lines are a fit to $\Delta E = aB$ for the first three data points. (h) The ratio of $B = 0$ slopes, Eq. (6), depends only on geometrical constraints. The theory (solid line) has no adjustable parameters. Data for other angles in [21].

applied field. In addition, the ultra-narrow linewidths in the SF system will allow the small energy shifts present in many-body interactions to be observed. As a rough estimate, the interaction energy of two such dipoles will exceed the SF FWHM of 77 μeV when the exciton density is greater than 230 μm^{-2}. Using a wavefunction size of approximately 10 nm, the critical density for exciton overlap in the 2D potential is 10 000 μm^{-2}. Therefore, the SF-bound exciton system could show sizable dipole-dipole interactions and may demonstrate coherent phenomena at reasonable exciton densities.

Acknowledgements. This material is based upon work supported by the National Science Foundation under Grant Number 1150647 and the National Science Foundation Graduate Research Fellowship under grant number DGE-1256082, and in part by the State of Washington through the University of Washington Clean Energy Institute. The Ioffe team has been partially supported by RFBR, RF President grant No. MD-5726.2015.2 and Dynasty foundation. A.K.R., A.L., and A.D.W. acknowledge partial support of Mercur Pr-2013-0001, DFG-TRR160, BMBF - Q.com-H 16KIS0109, and the DFH/UFA CDFA-05-06. We would like to acknowledge helpful discussions with John Schaibley, Pasqual Rivera, Xiaodong Xu, David Cobden and Matt McCluskey.

.

[1] S. Guha, J. M. DePuydt, M. A. Haase, J. Qiu, and H. Cheng, "Degradation of II-VI based blue-green light emitters," Applied Physics Letters **63**, 3107–3109 (1993).

[2] A. Colli, E. Pelucchi, and A. Franciosi, "Controlling the native stacking fault density in II-VI/III-V heterostructures," Applied Physics Letters **83**, 81–83 (2003).

[3] P. Caroff, J. Bolinsson, and J. Johansson, "Crystal phases in III–V nanowires: from random toward engineered polytypism," IEEE Journal of Selected Topics in Quantum Electronics **17**, 829–846 (2011).

[4] N. Akopian, G. Patriarche, L. Liu, J. C. Harmand, and V. Zwiller, "Crystal phase quantum dots," Nano Lett. **10**, 1198–1201 (2010).

[5] S. Assali, I. Zardo, S. Plissard, D. Kriegner, M. A. Verheijen, G. Bauer, A. Meijerink, A. Belabbes, F. Bechstedt, J. E. M. Haverkort, and E. P. A. M. Bakkers, "Direct band gap wurtzite gallium phosphide nanowires," *Nano Letters*, Nano Lett. **13**, 1559–1563 (2013).

[6] L. V. Butov, A. C. Gossard, and D. S. Chemla, "Macroscopically ordered state in an exciton system," Nature **418**, 751–754 (2002).

[7] A. A. High, A. K. Thomas, G. Grosso, M. Remeika, A. T. Hammack, A. D. Meyertholen, M. M. Fogler, L. V. Butov, M. Hanson, and A. C. Gossard, "Trapping indirect excitons

in a GaAs quantum-well structure with a diamond-shaped electrostatic trap," Phys. Rev. Lett. **103**, 087403 (2009).
[8] D. Snoke, S. Denev, Y. Liu, L. Pfeiffer, and K. West, "Long-range transport in excitonic dark states in coupled quantum wells," Nature **418**, 754–757 (2002).
[9] L. V. Butov, C. W. Lai, A. L. Ivanov, A. C. Gossard, and D. S. Chemla, "Towards Bose–Einstein condensation of excitons in potential traps," Nature **417**, 47 (2002).
[10] Yehiel Shilo, Kobi Cohen, Boris Laikhtman, Ken West, Loren Pfeiffer, and Ronen Rapaport, "Particle correlations and evidence for dark state condensation in a cold dipolar exciton fluid," Nat Commun **4** (2013), 10.1038/ncomms3335.
[11] A. A. High, A. T. Hammack, J. R. Leonard, Sen Yang, L. V. Butov, T. Ostatnický, M. Vladimirova, A. V. Kavokin, T. C. H. Liew, K. L. Campman, and A. C. Gossard, "Spin currents in a coherent exciton gas," Physical Review Letters **110** (2013), 10.1103/physrevlett.110.246403.
[12] M. M. Fogler, L. V. Butov, and K. S. Novoselov, "High-temperature superfluidity with indirect excitons in van der Waals heterostructures," Nature Communications **5** (2014), 10.1038/ncomms5555.
[13] A. V. Gorbunov and V. B. Timofeev, "Large-scale coherence of the bose condensate of spatially indirect excitons," JETP Letters **84**, 329 (2006).
[14] D. W. Snoke, "Coherence and optical emission from bilayer exciton condensates," Advances in Condensed Matter Physics **2011**, 1–7 (2011).
[15] B. Nelsen, R. Balili, D. W. Snoke, L. Pfeiffer, and K. West, "Lasing and polariton condensation: Two distinct transitions in GaAs microcavities with stress traps," Journal of Applied Physics **105**, 122414 (2009).
[16] R. Balili, B. Nelsen, D. W. Snoke, L. Pfeiffer, and K. West, "Role of the stress trap in the polariton quasiequilibrium condensation in GaAs microcavities," Phys. Rev. B **79**, 075319 (2009).
[17] A. A. High, J. R. Leonard, A. T. Hammack, M. M. Fogler, L. V. Butov, A. V. Kavokin, K. L. Campman, and A. C. Gossard, "Spontaneous coherence in a cold exciton gas," Nature **483**, 584–588 (2012).
[18] A. Amo, T. C. H. Liew, C. Adrados, R. Houdre, E. Giacobino, A. V. Kavokin, and A. Bramati, "Exciton-polariton spin switches," Nature Photonics **4**, 361–366 (2010).
[19] H. S. Nguyen, D. Vishnevsky, C. Sturm, D. Tanese, D. Solnyshkov, E. Galopin, A. Lemaître, I. Sagnes, A. Amo, G. Malpuech, and J. Bloch, "Realization of a double-barrier resonant tunneling diode for cavity polaritons," Phys. Rev. Lett. **110**, 236601 (2013).
[20] E. Kammann, T. C. H. Liew, H. Ohadi, P. Cilibrizzi, P. Tsotsis, Z. Hatzopoulos, P. G. Savvidis, A. V. Kavokin, and P. G. Lagoudakis, "Nonlinear optical spin Hall effect and long-range spin transport in polariton lasers," Phys. Rev. Lett. **109**, 036404 (2012).
[21] See Supplemental Material at [URL will be inserted by publisher] for details on sample growth, an overview of the optical spectroscopy system, details of the linewidth measurements, data for the angle resolved experiment, derivation of the magneto-Stark Hamiltonian and an explanation of the g-factor analysis.
[22] J. Kasai and M. Kawata, "Microphotoluminescence of oval defects in a GaAs layer grown by molecular beam epitaxy," Applied Physics Letters **73**, 2012–2014 (1998).
[23] J. Lähnemann, U. Jahn, O. Brandt, T. Flissikowski, P. Dogan, and H. T. Grahn, "Luminescence associated with stacking faults in GaN," Journal of Physics D: Applied Physics **47**, 423001 (2014).
[24] R. E. Algra, M. A. Verheijen, M. T. Borgstrom, L. F. Feiner, G. Immink, W. J. P. van Enckevort, E. Vlieg, and E. P. A. M. Bakkers, "Twinning superlattices in indium phosphide nanowires," Nature **456**, 369–372 (2008).
[25] A. Belabbes, C. Panse, J. Furthmüller, and F. Bechstedt, "Electronic bands of III-V semiconductor polytypes and their alignment," Phys. Rev. B **86**, 075208 (2012).
[26] D. Spirkoska, J. Arbiol, A. Gustafsson, S. Conesa-Boj, F. Glas, I. Zardo, M. Heigoldt, M. H. Gass, A. L. Bleloch, S. Estrade, M. Kaniber, J. Rossler, F. Peiro, J. R. Morante, G. Abstreiter, L. Samuelson, and Fontcuberta, "Structural and optical properties of high quality zinc-blende/wurtzite GaAs nanowire heterostructures," Phys. Rev. B **80**, 245325 (2009).
[27] M. Heiss, S. Conesa-Boj, J. Ren, H. H. Tseng, A. Gali, A. Rudolph, E. Uccelli, F. Peiró, J. R. Morante, D. Schuh, E. Reiger, E. Kaxiras, J. Arbiol, and Fontcuberta, "Direct correlation of crystal structure and optical properties in wurtzite/zinc-blende GaAs nanowire heterostructures," Phys. Rev. B **83**, 045303 (2011).
[28] J. Lähnemann, O. Brandt, U. Jahn, C. Pfüller, C. Roder, P. Dogan, F. Grosse, A. Belabbes, F. Bechstedt, A. Trampert, and L. Geelhaar, "Direct experimental determination of the spontaneous polarization of GaN," Phys. Rev. B **86**, 081302 (2012).
[29] N. Vainorius, S. Lehmann, D. Jacobsson, L. Samuelson, K. A. Dick, and M. E. Pistol, "Confinement in thickness-controlled GaAs polytype nanodots," Nano Lett. **15**, 2652–2656 (2015).
[30] K. K. Fung, N. Wang, and I. K. Sou, "Direct observation of stacking fault tetrahedra in ZnSe/GaAs(001) pseudomorphic epilayers by weak beam dark-field transmission electron microscopy," Applied Physics Letters **71**, 1225–1227 (1997).
[31] N. Wang, K. K. Fung, and I. K. Sou, "Direct observation of stacking fault nucleation in the early stage of ZnSe/GaAs pseudomorphic epitaxial layer growth," Applied Physics Letters **77**, 2846–2848 (2000).
[32] P. Corfdir and P. Lefebvre, "Importance of excitonic effects and the question of internal electric fields in stacking faults and crystal phase quantum discs: The model-case of GaN," Journal of Applied Physics **112**, 053512 (2012).
[33] H. Kakibayashi, F. Nagata, Y. Katayama, and Y. Shiraki, "Structure analysis of oval defect on molecular beam epitaxial GaAs layer by cross-sectional transmission electron microscopy observation," Japanese Journal of Applied Physics **23**, L846–L848 (1984).
[34] Teruo Komatsu, "Optical properties of excitons confined two-dimensionally in a stacking fault plane in BiI3," Journal of Luminescence **40-41**, 495–496 (1988).
[35] S. V. Poltavtsev, Yu Efimov, Yu Dolgikh, S. A. Eliseev, V. V. Petrov, and V. V. Ovsyankin, "Extremely low inhomogeneous broadening of exciton lines in shallow (In,Ga)As/GaAs quantum wells," Solid State Communications **199**, 47–51 (2014).
[36] A. M. Graham, P. Corfdir, M. Heiss, S. Conesa-Boj, E. Uccelli, Fontcuberta, and R. T. Phillips, "Exciton localization mechanisms in wurtzite/zinc-blende GaAs nanowires," Phys. Rev. B **87**, 125304 (2013).
[37] B. Pal, K. Goto, M. Ikezawa, Y. Masumoto, P. Mohan, J. Motohisa, and T. Fukui, "Type-II behavior in wurtzite InP/InAs/InP core-multishell nanowires," Applied Physics Letters **93**, 073105 (2008).
[38] G. Signorello, E. Lörtscher, P. A. Khomyakov, S. Karg, D. L. Dheeraj, B. Gotsmann, H. Weman, and H. Riel, "Inducing a

direct-to-pseudodirect bandgap transition in wurtzite GaAs nanowires with uniaxial stress," Nature Communications **5** (2014), 10.1038/ncomms4655.
[39] D. Spirkoska, A. L. Efros, W. R. L. Lambrecht, T. Cheiwchanchamnangij, A. F. Morral, and G. Abstreiter, "Valence band structure of polytypic zinc-blende/wurtzite GaAs nanowires probed by polarization-dependent photoluminescence," Phys. Rev. B **85**, 045309 (2012).
[40] Our sample is non-magnetic and we use linearly polarized light to avoid dynamic polarization of nuclear spins.
[41] R. S. Knox, *Theory of Excitons - Supplement 5 Solid State Physics* (Academic Press, New York, New York, 1963).
[42] Experimentally, the NA = 0.7 objective lens collects luminescence from a range of angles. In our system, light is collected from excitons momenta within 7% of $\hbar K_x$ in Eq. (2).
[43] E. F. Gross, B. P. Zakharchenya, and O. V. Konstantinov, "Effect of magnetic field inversion in spectra of exciton absorption in CdSe crystal," Sov. Phys. Solid State **3**, 221 (1961).
[44] D. G. Thomas and J. J. Hopfield, "A magneto-Stark effect and exciton motion in CdS," Phys. Rev. **124**, 657–665 (1961).
[45] U. Jahn, J. Lähnemann, C. Pfüller, O. Brandt, S. Breuer, B. Jenichen, M. Ramsteiner, L. Geelhaar, and H. Riechert, "Luminescence of GaAs nanowires consisting of wurtzite and zinc-blende segments," Physical Review B **85** (2012), 10.1103/physrevb.85.045323.
[46] R. J. Warburton, C. Schulhauser, D. Haft, C. Schäflein, K. Karrai, J. M. Garcia, W. Schoenfeld, and P. M. Petroff, "Giant permanent dipole moments of excitons in semiconductor nanostructures," Phys. Rev. B **65**, 113303 (2002).
[47] Y. G. Chai, Y-c. Pao, and T. Hierl, "Elimination of "pair" defects from GaAs layers grown by molecular beam epitaxy," Applied Physics Letters **47**, 1327–1329 (1985).
[48] J. E. M. Haverkort, M. P. Schuwer, M. R. Leys, and J. H. Wolter, "Spatial variations of photoluminescence line broadening around oval defects in GaAs/AlGaAs multiple quantum wells," Semiconductor Science and Technology **7** (1992).
[49] G. L. Bir and G. E. Pikus, *Symmetry and strain-induced effects in semiconductors* (Halsted Press, 1974).
[50] G. F. Koster, J. O. Dimmock, and R. G. Wheeler, *Properties of the thirty-two point groups* (M.I.T. Press, 1963).
[51] M. S. Dresselhaus, G. Dresselhaus, and A. Jorio, *Group Theory: Application to the Physics of Condensed Matter*, 2008th ed. (Springer, Berlin, Germany, 2008).
[52] J. L. Birman, "Some selection rules for band-band transitions in wurtzite structure," Phys. Rev. **114**, 1490–1492 (1959).
[53] G. Dresselhaus, "Spin-orbit coupling effects in zinc blende structures," Phys. Rev. **100**, 580–586 (1955).
[54] C. Herring, "Effect of time-reversal symmetry on energy bands of crystals," Phys. Rev. **52**, 361–365 (1937).
[55] R. J. Elliott, "Spin-orbit coupling in band theory–character tables for some "double" space groups," Phys. Rev. **96**, 280–287 (1954).
[56] G. Sallen, B. Urbaszek, M. M. Glazov, E. L. Ivchenko, T. Kuroda, T. Mano, S. Kunz, M. Abbarchi, K. Sakoda, D. Lagarde, A. Balocchi, X. Marie, and T. Amand, "Dark-bright mixing of interband transitions in symmetric semiconductor quantum dots," Phys. Rev. Lett. **107**, 166604 (2011).
[57] G. Burns, *Introduction to group theory with applications: materials science and technology* (Academic Press, 1977).
[58] E. L. Ivchenko and G. E. Pikus, *Superlattices and other heterostructures: symmetry and optical phenomena* (Springer, 1997).
[59] Z. Ikonic, V. Milanovic, and D. Tjapkin, "Valence subband structure of [100]-, [110]-, and [111]-grown GaAs-(Al,Ga)As quantum wells and the accuracy of the axial approximation," Phys. Rev. B **46**, 4285–4288 (1992).